The measurement of the coordinate along the sense wire with decoupling capacitors

M. Agnello[a], *E. Botta[b], L. Busso[c], D. Calvo[b], P. Cerello[b], C. Fanara[a], A. Feliciello[b].

[a] Politecnico di Torino and INFN, Sez. di Torino, Torino, Italy.
[b] INFN, Sez. di Torino, Torino, Italy.
[c] Dip. di Fisica Generale, Università di Torino, and INFN, Sez. di Torino, Torino, Italy.

Abstract

It is well known that drift chambers can provide a good spatial resolution (a few tenths of a millimeter or even better) on the coordinate along the drift direction. On the other hand, the measurement of the coordinate along the sense wire by charge division appears to be limited by the electronic noise and the stability of the electronic chain.

If the sense wire must be kept at high voltage, decoupling capacitors are needed and cause a systematic coordinate compression. The performance of the charge division method in these conditions is discussed in the framework of a simplified model and compared to experimental data.

The compression error can be kept at the same level of the electronic noise, about 0.55% of the sense wire length.

PACS 29.07.50.QX
Keywords: charge division, drift chambers, hypernuclei.

1 Introduction

The main goal of the FINUDA experiment, that will be installed at the *DAΦNE* e^+e^- collider which is being built at the *INFN Laboratori Nazionali di Frascati*, is high resolution hypernuclear spectroscopy [1].

Two layers of eight Low Mass Drift Chambers (*LMDCs*) each are the central part of the tracking system: they will be assembled to form two coaxial octagonal based prisms. The internal point of the particles, as close as possible to the target,

*Corresponding author. Fax: +39 11 6707324, e–mail: botta@to.infn.it.

is measured by a layer of double sided silicon μ-strips, while the external point is provided by a complex array of straw tubes. The Low Mass Drift Chambers will measure two intermediate points, providing a $100\,\mu m$ resolution in the (ρ, ϕ) plane and a much more coarse resolution (about 1% of the wire length) on the coordinate along the wire.

The main factors affecting the experimental resolution are the multiple scattering, caused by the material along the particle path, and the precision on the track points measurement.

The momentum resolution to be achieved requires a minimum amount of material along the particle path, in order to minimize the multiple scattering effect: for this reason the drift chambers will be filled with a $He - iC_4H_{10}(70\% - 30\%)$ gas mixture. Since high localization precision is required only in the (ρ, ϕ) plane the LMDCs have only one drift layer and are equipped with very thin mylar windows. The coordinate along the sense wire is obtained by charge division: this method is particularly suitable since it doesn't require any additional material along the particle path.

The requirement of low mass is particularly stringent on the detectors located along the particle trajectory, while it can be partially released for those measuring the initial and final points.

A detailed discussion of the FINUDA experimental layout can be found in ref. [2], [3].

2 The Charge Division Method

The charge division method has already been discussed in various papers [4, 5, 6]: the electrons produced in the ionization process by a charged particle crossing the sensitive gas volume drift towards the sense wire, where they are amplified in avalanches and collected. The charge pulses coming from each end of the sense wire must be measured, since the collection point along the wire is proportional to their asymmetry. The accuracy is limited by the electronic noise and by the stability of the electronic chain. When an avalanche is generated in a point P along the wire (fig. 1), the electron current i is divided in a left and a right component (i_L and i_R) in such a way that, if the capacitors are neglected:

$$\frac{i_L}{i_R} = \frac{R_R + R_i}{R_L + R_i} = \frac{\rho(\frac{L}{2} - z) + R_i}{\rho(\frac{L}{2} + z) + R_i}$$

where L, ρ, R_i and z are respectively the length and resistivity of the wire, the amplifier impedance and the coordinate along the wire in a reference frame centered in the middle of the wire.

The following, well known formula is obtained:

$$z_{real} = \frac{Q_R - Q_L}{Q_R + Q_L}\left(\frac{R_i}{\rho} + \frac{L}{2}\right) = \frac{Q_R - Q_L}{Q_R + Q_L}K = \frac{\Delta R}{R_t}K$$

where $Q_{L,R} = \int i_{L,R} dt$, $R_t = (2R_i + \rho L)$ and $\Delta R \equiv R_L - R_R$.

When the sense wire must be kept at high voltage, as in our experimental conditions, a decoupling capacitor is needed and a z compression arises: this effect must therefore be evaluated and corrected for. The capacitance value is chosen in such a way that the energy stored in the capacitor is small enough to avoid a wire breaking.

The experimental tests on a drift chamber prototype ($PLMDC$) are described in the following and their results are compared to the predictions coming from a simplified model.

3 Experimental apparatus

A prototype of the drift chambers for the FINUDA experiment ($PLMDC$) was tested in November 94 and in June 95 at the CERN PS with a $5\,GeV/c$ π^- beam [7]: a scheme of the experimental setup is shown in fig. 2.

The prototype was filled with a He-iC_4H_{10} $(70\% - 30\%)$ gas mixture and had the following geometrical and electrical characteristics:

1. wire length: $L = 118\ cm$;
2. sensitive planar surface: $115 \times 55\,cm^2$;
3. drift cell length: $DL = 2.5\ cm$;
4. drift cell thickness: $DT = 0.6\ cm$ gap;
5. sense wire resistivity: $\rho = 17.71\ \Omega/cm$;
6. amplifier input impedance: $R_i = 112\ \Omega$;
7. decoupling capacitance: $C = 2.2\ nF$;

The time constant τ and the factor K were: $\tau = (\rho L + 2R_i)C/2 = 2.54\ \mu s$ and $K = (R_i/\rho + L/2) = 65.3\ cm$, according to Radeka's approximation [5] for a good charge division method performance.

The $PLMDC$ was mounted on a mechanical support which could be moved along the x and z directions and also rotated around the x-axis. For the measurements described here, the $PLMDC$ was placed between two small drift chambers, filled with the same gas mixture, which gave the two beam perpendicular coordinates (x and z) for all the particles crossing the $PLMDC$. A more detailed description of the apparatus can be found in ref. [8].

The beam size along the wire coordinate was about $0.4\,cm$. The ADC time gate was opened by the coincidence signals coming from the amplifiers placed on the two sides of the sense wire for an integration time T.

Data were collected with the $PLMDC$ placed in different positions and with variable orientations with respect to the incident beam: in particular, results with a perpendicular incoming beam at different values of the coordinate along the sense wire are discussed in the following.

4 A Simplified Model

A simplified model can be a guide line and could allow to estimate the method validity with limited decoupling capacitor values.

Let's suppose the electron collection generates a squared current pulse of amplitude I and duration t_1. During this time interval, referring to fig.3, where R_i is the amplifier input impedance and R_L and R_R the left and right wire resistances, the following equations hold:

$$\begin{cases} I = i_R + i_L \\ i_L R_L + V_{CL} + i_L R_i = i_R R_R + V_{CR} + i_R R_i \end{cases}$$

Eliminating i_L and differentiating, with $R_t \equiv 2R_i + R_L + R_R$, the result is the differential equation:

$$\frac{di_R}{dt} + \frac{2}{R_t C} i_R - \frac{I}{R_t C} = 0$$

which, solved, gives for the left and right currents the values:

$$i_{R,L} = \frac{I}{2}\left[1 \pm \frac{\Delta R}{R_t} e^{-\frac{t}{\tau}}\right]$$

where $\tau \equiv R_t C/2$ and $\Delta R \equiv R_R - R_L$.

The collected charge up to time t_1 is given by:

$$Q^1_{R,L} = \int_0^{t_1} i_{R,L} dt = \frac{I}{2}\left[t_1 \pm \frac{\Delta R}{R_t} \tau (1 - e^{-t_1/\tau})\right] \tag{1}$$

Since the current is different on the left and right side, at the end of the pulse there is a ΔV voltage difference between the left and right capacitor:

$$\Delta V = V_{CR} - V_{CL} = \frac{I}{2} \Delta R (1 - e^{-t_1/\tau}) \tag{2}$$

This voltage difference originates a current $i(t)$ for $t > t_1$, given by:

$$i(t) = \frac{I}{2}\frac{\Delta R}{R_t}(1 - e^{-t_1/\tau}) e^{-(t-t_1)/\tau}, \qquad t > t_1 \tag{3}$$

At the time $t_2 > t_1$ a charge $Q(t_2)$ is collected:

$$Q(t_2) = \frac{I\tau}{2}\frac{\Delta R}{R_t}(1 - e^{-t_1/\tau})(1 - e^{-(t_2-t_1)/\tau}) \tag{4}$$

The net charge on the right and left side is therefore:

$$Q_{R,L} = Q^1_{R,L} \mp Q(t_2) = \frac{I}{2}\left[t_1 \mp \frac{\Delta R}{R_t}\tau(1 - e^{-t_1/\tau})e^{-(t_2-t_1)/\tau}\right] \tag{5}$$

The coordinate along the wire (z) at the end of the pulse ($t = t_1$)is given by:

$$z_{t_1} = \frac{\int_0^{t_1}(i_R - i_L)dt}{\int_0^{t_1}(i_R + i_L)dt}\left(\frac{L}{2} + \frac{R_i}{\rho}\right) = K\frac{\Delta R}{R_t}\frac{\tau}{t_1}\left(1 - e^{-\frac{t_1}{\tau}}\right) \tag{6}$$

The real value (z_{real}) is, from (6):

$$z_{real} = K\frac{\Delta R}{R_t} = \frac{z_{t_1}}{(\tau/t_1)(1 - e^{-t_1/\tau})} \sim \frac{z_{t_1}}{(1 - t_1/2\tau)} \quad (t_1 \ll \tau) \tag{7}$$

The relative systematic error on the coordinate is therefore:

$$\frac{\Delta z}{z_{real}} \equiv \frac{|z_{t_1} - z_{real}|}{z_{real}} = \left[1 - \frac{\tau}{t_1}\left(1 - e^{-t_1/\tau}\right)\right] \sim \frac{t_1}{2\tau} \tag{8}$$

In order to have a compression error of 1% of the wire length ($L = 2z_{Max}$), either the pulse duration must be at most $\tau/25 \sim 100\,ns$ or the integration time must be not longer than 100 ns.

In general, however, the current $i(t)$ flowing for $t > t_1$ can't be neglected. Therefore, if the squared pulse duration is t_1 and the integration time is $t_2 > t_1$, the z coordinate is given by:

$$z_{t_2} = K\frac{\int_{t_0}^{t_1} i_R dt - \int_{t_0}^{t_1} i_L dt + 2\int_{t_1}^{t_2} i dt}{\int_{t_0}^{t_1} i_R dt + \int_{t_0}^{t_1} i_L dt} = K\frac{\Delta R}{R_t}\frac{\tau}{t_1}\left(1 - e^{-t_1/\tau}\right)e^{-(t_2-t_1)/\tau} = \tag{9}$$

$$= K\frac{\Delta R}{R_t}\frac{\tau}{t_1}\left(e^{t_1/\tau} - 1\right)e^{-t_2/\tau} \tag{10}$$

Therefore:

$$z_{real} = \frac{z_{t_2}}{(\tau/t_1)\left(e^{t_1/\tau} - 1\right)e^{-t_2/\tau}} \tag{11}$$

and the systematic compression factor is:

$$\frac{\Delta z}{z_{real}} \equiv \frac{|z_{t_2} - z_{real}|}{z_{real}} = 1 - \frac{\tau}{t_1}\left(e^{-t_1/\tau} - 1\right)e^{-(t_2-t_1)/\tau} \tag{12}$$

Table 1: The meaning of the different symbols referring to the z coordinate.

Symbol	Meaning
z_{t_1}	Model prediction for a gate t_1 coincident with the signal duration
z_{t_2}	Model prediction for a gate t_2 greater than the signal duration t_1
z_{real}	Real value to be obtained
z_{rec}	Reconstructed value (before the correction)
z_{cor}	Reconstructed value (after the correction)
z_{geom}	Geometrical value to which the $PLMDC$ or the ^{106}Ru source were positioned

5 Results

The aim of the experimental tests was twofold: to evaluate the dependence of the compression factor on the ADC gate width and to verify the accuracy of a software correction.

The presented data have been collected at two different positions along the sense wire ($z_{geom} = 30\ cm$ and $z_{geom} = 44\ cm$). Fig. 4 shows the measured (black triangles) and corrected (white triangles) values for the coordinate as a function of the ADC time gate. The solid lines show the model predictions for a squared signal of 50 ns duration (t_1), which is our approximation to the effective experimental conditions, in which the duration for perpendicularly incident particles is about 80 ns but the shape is not squared. The dashed lines are the geometrical values to be obtained after the correction. There is still a disagreement with respect to the geometrical z value: fig. 5 shows the residual systematic error as a percentage of the sense wire length. The effect is at most of the order of 2.5%, much smaller than before the correction but still too large compared to the required resolution of about 1%.

The model is more suitable to describe the data at short ADC gate values, while it is getting worse as the gate width increases, because of its intrinsic limits: it was developed in the approximation of a squared pulse with fixed duration, corresponding to perpendicularly incident particles.

Moreover, there seems to be a z dependence of the correction factor, in contradiction with a naive expectation.

The relative systematic error ($\Delta z/z \equiv |z_{geom} - z_{rec}|/z_{geom}$) caused by the decoupling capacitor, according to the analytical calculation (full line) is shown in fig.6 as a function of the gate time width and compared to the experimental data at $z = 30\ cm$ (black triangles) and at $z = 44\ cm$ (white triangles): in case there were no z dependence, the data at different coordinates should lie on the model prediction.

The unexpected dependence on the position was investigated more carefully in a dedicated laboratory test on the $PLMDC$, using a 6 mm collimated ^{106}Ru source, taking two fixed gate widths (100 ns and 800 ns) and testing the correlation between the reconstructed coordinate (z_{rec}) and the geometrical value (z_{geom}). The result (fig. 7) shows a good agreement between the model (full line) and the experimental data for a 100 ns ADC gate, while for a 800 ns ADC gate the experimental data do not lie on a straight line, as it is expected in case of no z dependence: the model prediction (dashed line) shows a disagreement of a few percent.

The correction factor to be applied to the reconstructed z in order to get the true value, derived from the data, is displayed in fig. 8; at 800 ns it sensibly increases with the coordinate and it is quite far from the constant value expected from the model (dashed line). On the other hand, at 100 ns, the data are consistent with a constant value within less than 1%.

The required performance in the z coordinate measurement ($\sigma_z/L_{wire} \sim 1\%$) is not compatible with the disagreement at 800 ns. Moreover, an offline correction with a three variable function (z, t_1 and t_2) is not suitable and would require a very complicated calibration procedure: an ADC with 100 ns gate width would be much simpler and safer.

Finally, the intrinsic fluctuation on the value of the correction factor, due to the electronic noise, slightly increases with the ADC time gate: the precision on the single measurement of the z coordinate is therefore worsening as the ADC time gate increases. Fig. 9 shows the statistical error σ_z divided by the wire length at different z for an ADC gate of 100 ns and 800 ns (black and white triangles): the resolution is well under the required value (1%) for a 100 ns gate.

6 Conclusions

The performance of the charge division method for the measurement of the coordinate along the sense wire when a decoupling capacitor is included at the front-end has been discussed. The systematic compression induced by the presence of the capacitor, contrary to the expectations, weakly depends on the hit position along the wire; furthermore, it is a function of the ADC time gate and of the signal duration.

The three parameter dependence makes it very difficult to keep the measurement under control with a dedicated calibration at the required sensitivity of about 1%, unless the ADC time gate is short enough.

As a consequence, a hardware option to minimize the ADC time gate and to make it driven by the arrival time of the signal is needed: this approach intrinsically takes into account the effect of the capacitors, directly providing the compensated z value, and allows to reach a resolution of $\sigma_z/L_{wire} \sim 0.55\%$.

7 Acknowledgements

The authors wish to thank Prof. T. Bressani for many helpful discussions. Mr. A. Carnino and Mr. D. Bergo are gratefully acknowledged for their collaboration during the laboratory tests.

References

[1] The FINUDA Collaboration, *Report*, INFN Report LNF-93/021 (1993)

[2] The FINUDA Collaboration, *Report*, INFN Report LNF-95/024 (1995)

[3] L. Maiani et al *The second* DAΦNE *HandBook* ***I-II***, LNF-INFN (1995)

[4] J. Alberi and V. Radeka, *IEEE Trans. Nucl. Sci.* **23** 251 (1976)

[5] V. Radeka, *IEEE Trans. Nucl. Sci.* **26** 225 (1979)

[6] W. Blum and L. Rolandi, *Particle Detection with Drift Chambers*, Springer-Verlag, 1993

[7] M. Agnello et al. accepted by *Nucl. Instr. and Methods* **A**, ref. NIMA 11043.

[8] M.Agnello et al. *Nucl. Instr. and Methods* **A367**, 100 (1995)

List of Tables

List of Figures

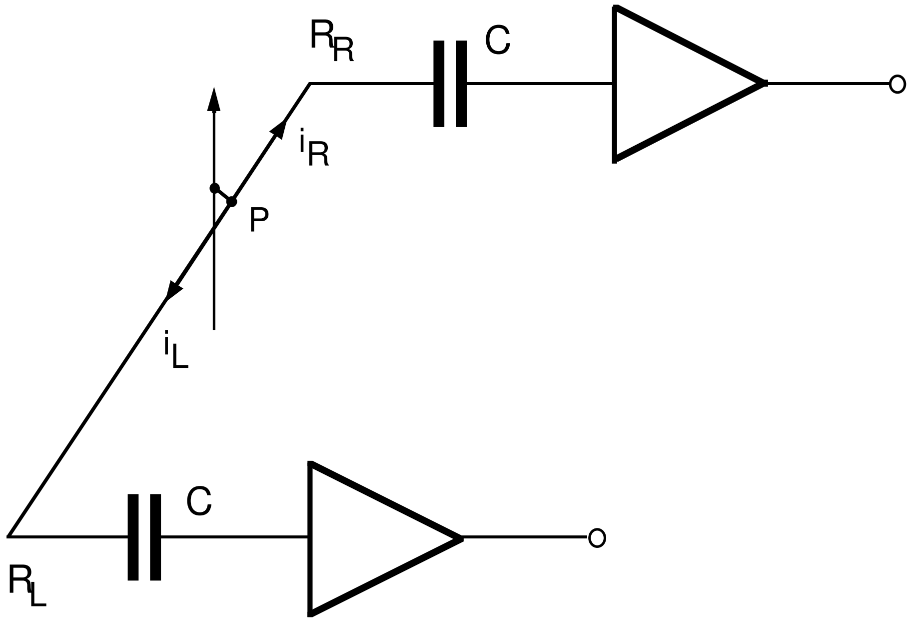

Figure 1: The electrical scheme of the sense wire and its front-end electronics. The signal from the charged track is collected in P.

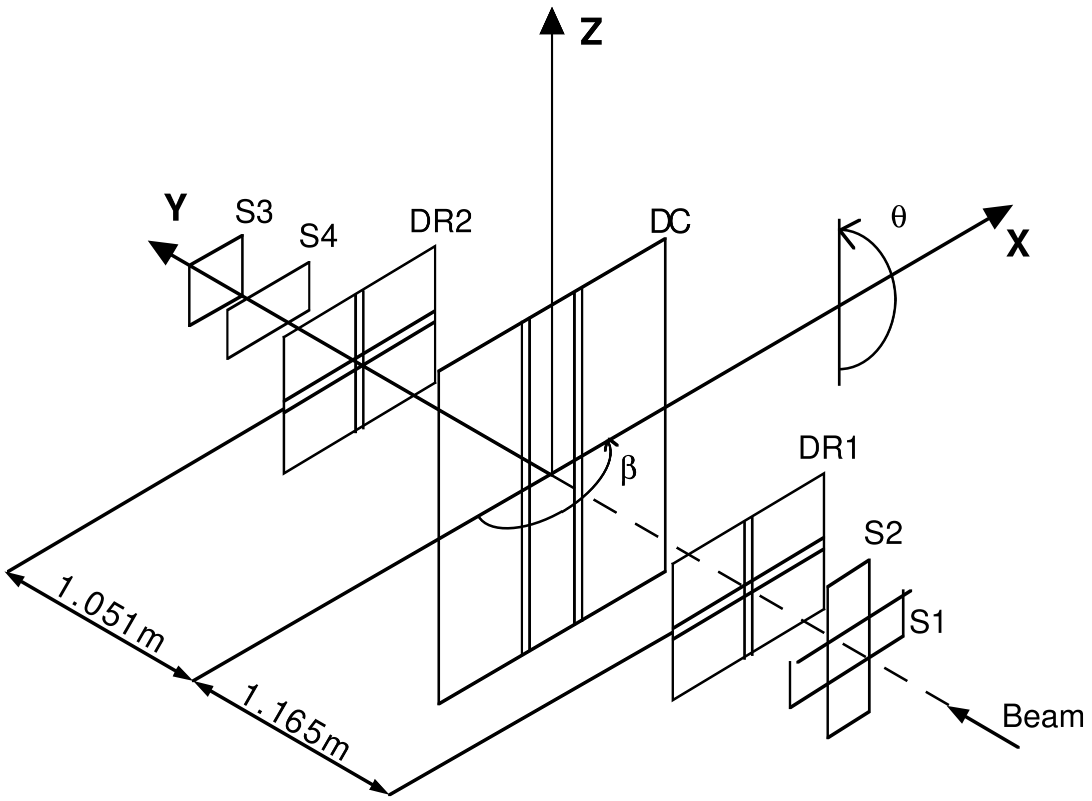

Figure 2: The experimental setup during the beam test at the CERN PS. DC is the protype under test. The small drift chambers DR1 and DR2 determine the beam position. The scintillators S1, S2, S3, S4 define the trigger condition.

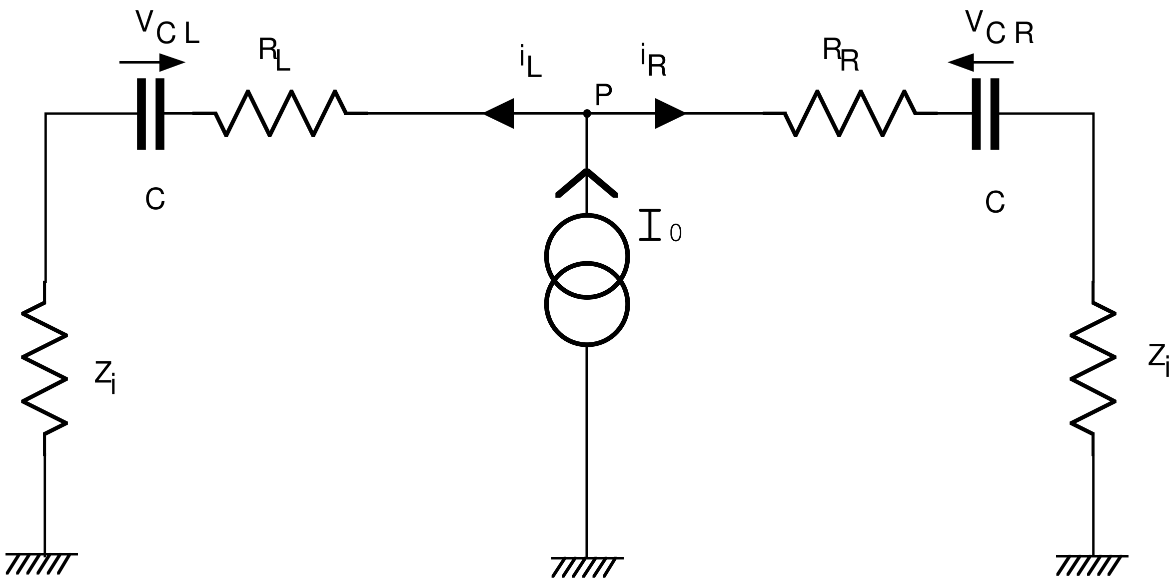

Figure 3: The electrical circuit according to the simplified model. The charge collected in P is considered to be equivalent to an ideal current generator, supplying a current I_0, which then splits into i_L and i_R through the resistances R_L and R_R and the amplifier input impedances z_i. At the end of the pulse, the two capacitors C are charged at different voltage (V_{CL} and V_{CR}).

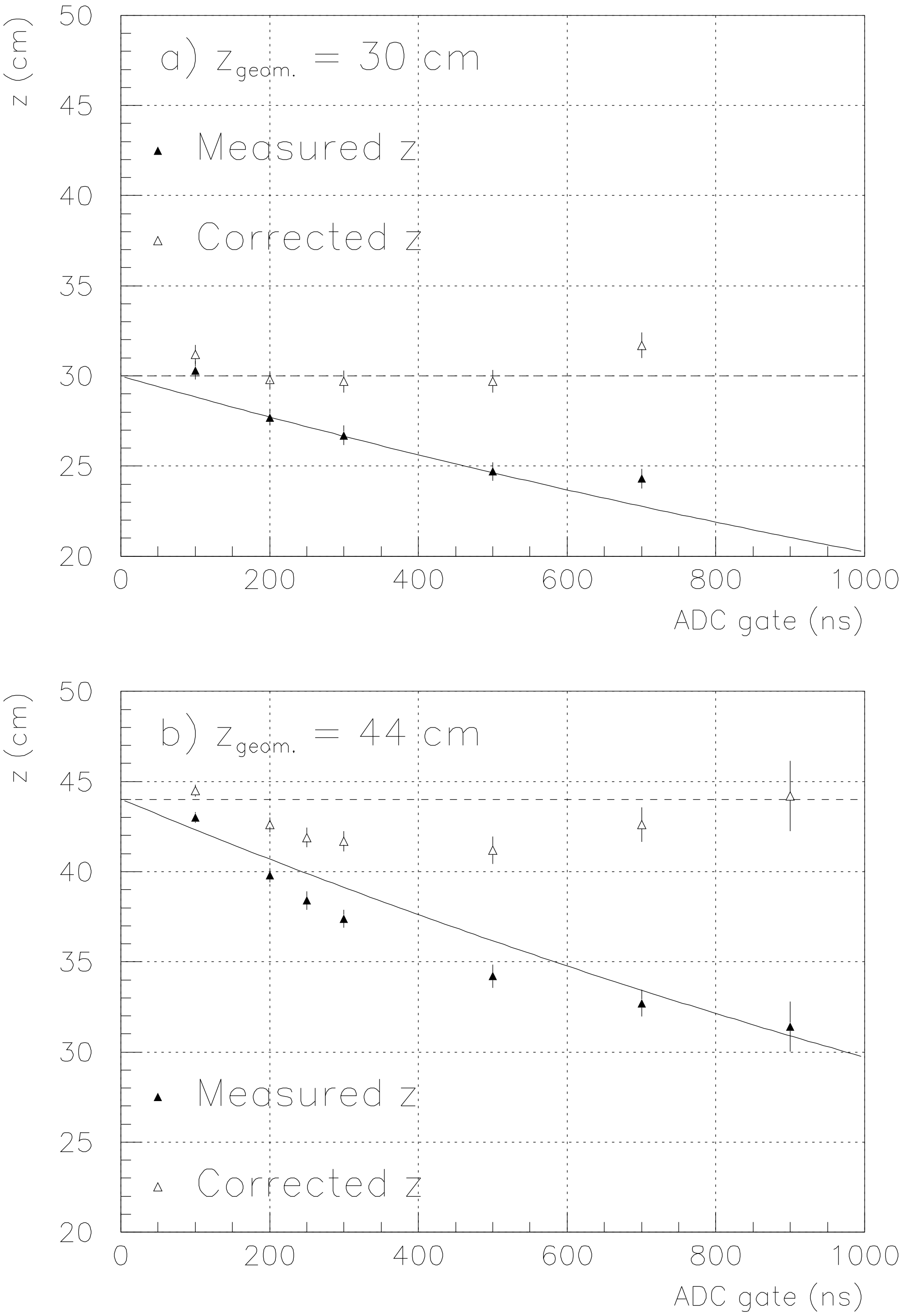

Figure 4: The measured and corrected z, according to the model, at $z_{geom} = 30\ cm$ (a) and $z_{geom} = 44\ cm$ (b) as a function of the ADC time gate width. The full line is the model prediction, while the dashed line is the geometrical value.

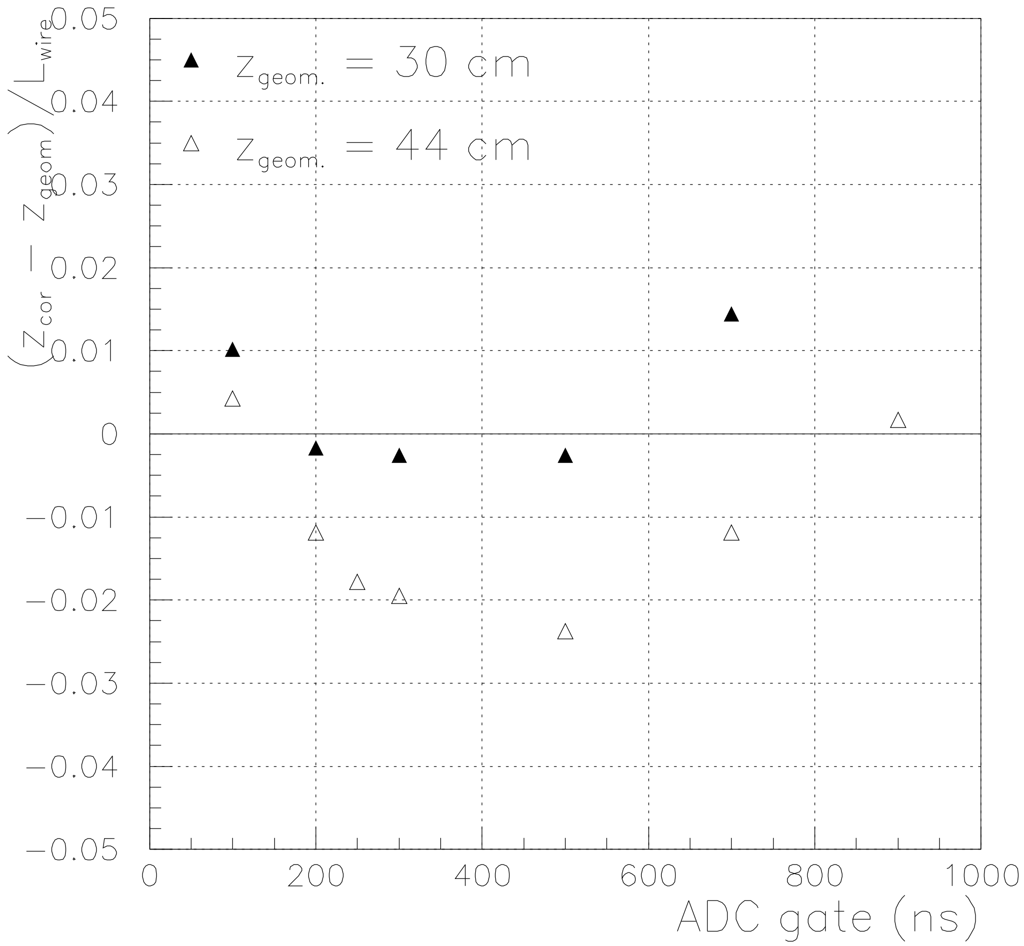

Figure 5: The residual systematic error after the correction: $(z_{cor} - z_{geom})/L_{wire}$ as a function of the ADC gate width.

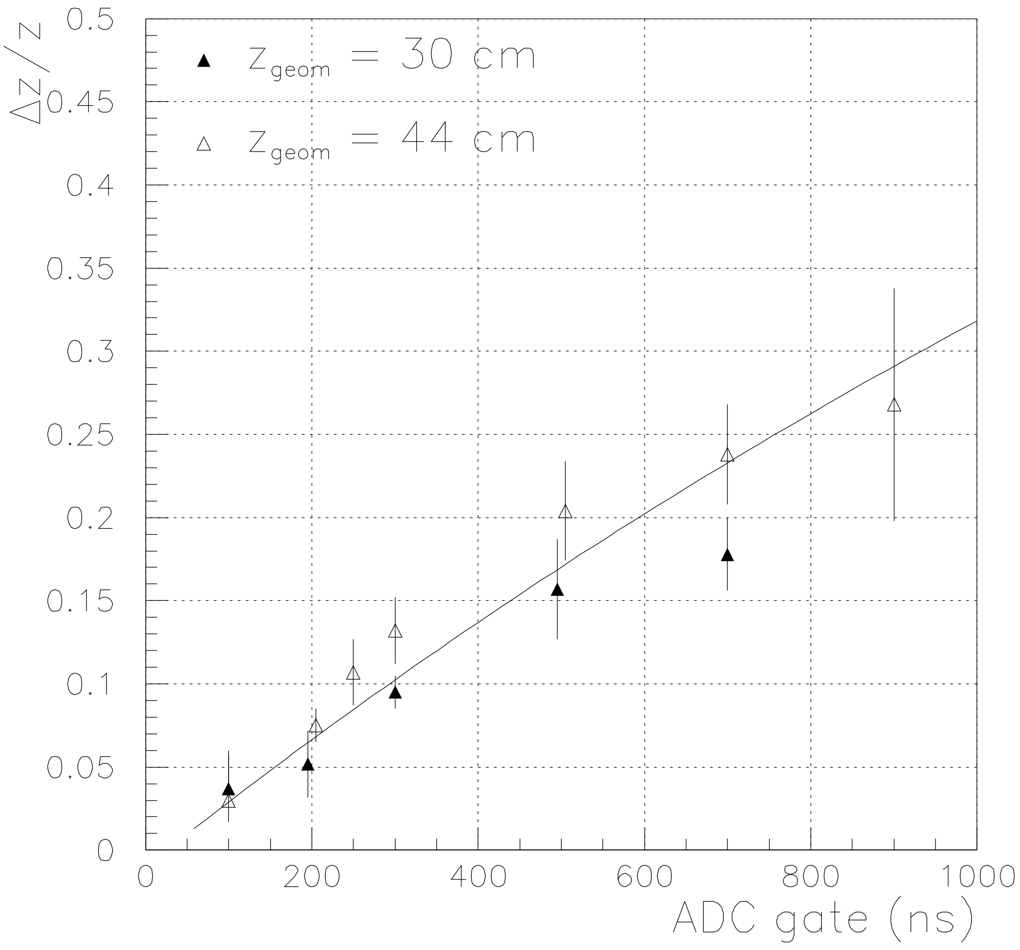

Figure 6: The ratio $\Delta z/z = |z_{rec} - z_{geom}|/z_{geom}$ as a function of the ADC time gate for $z = 30\ cm$ (black triangles) and $z = 44\ cm$ (white triangles). The full line shows the model prediction, independent of z.

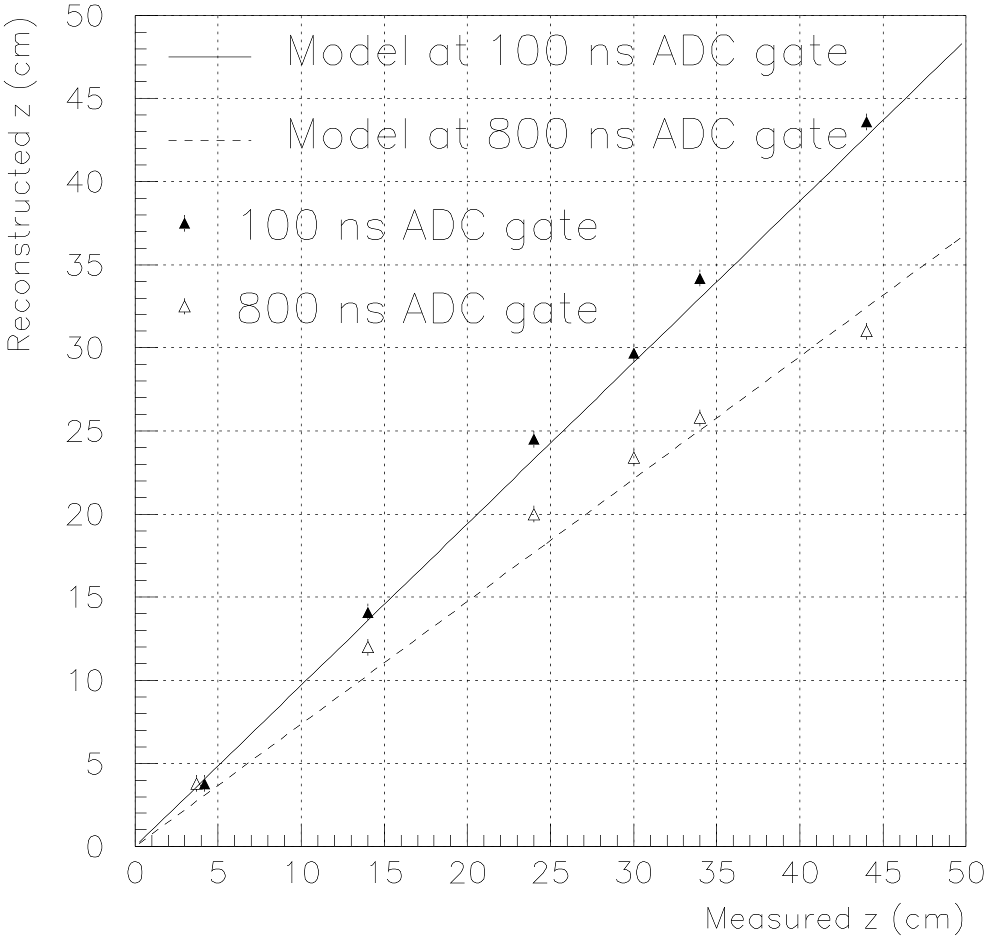

Figure 7: The correlation between the reconstructed (z_{rec}) and the geometrical (z_{geom}) coordinate for an ADC gate of 100 ns and 800 ns (black and white triangles). The data are compared to the model predictions for a gate of 100 ns (full line) and 800 ns (dashed line).

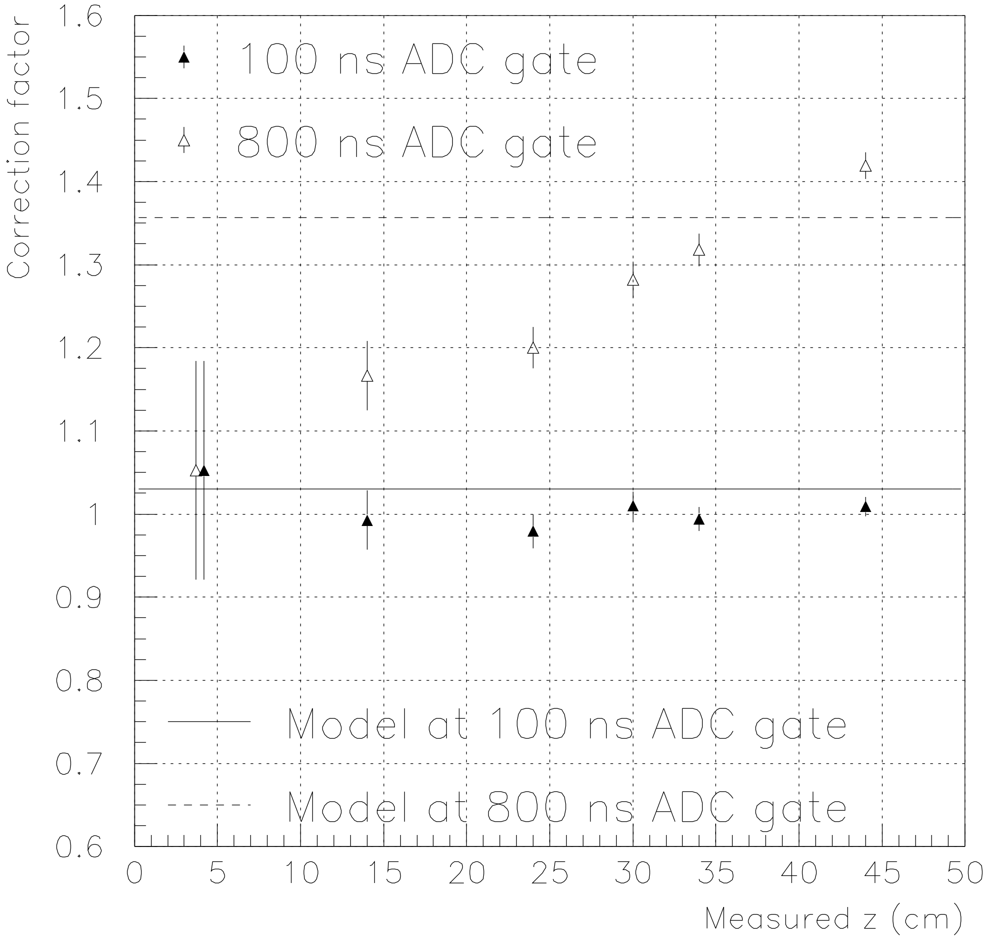

Figure 8: The correction factor as a function of the position along the sense wire at fixed ADC time gate: experimental data at 100 ns and 800 ns ADC gate width (black and white triangles) and model predictions at 100 ns and 800 ns ADC gate width (full and dashed lines).

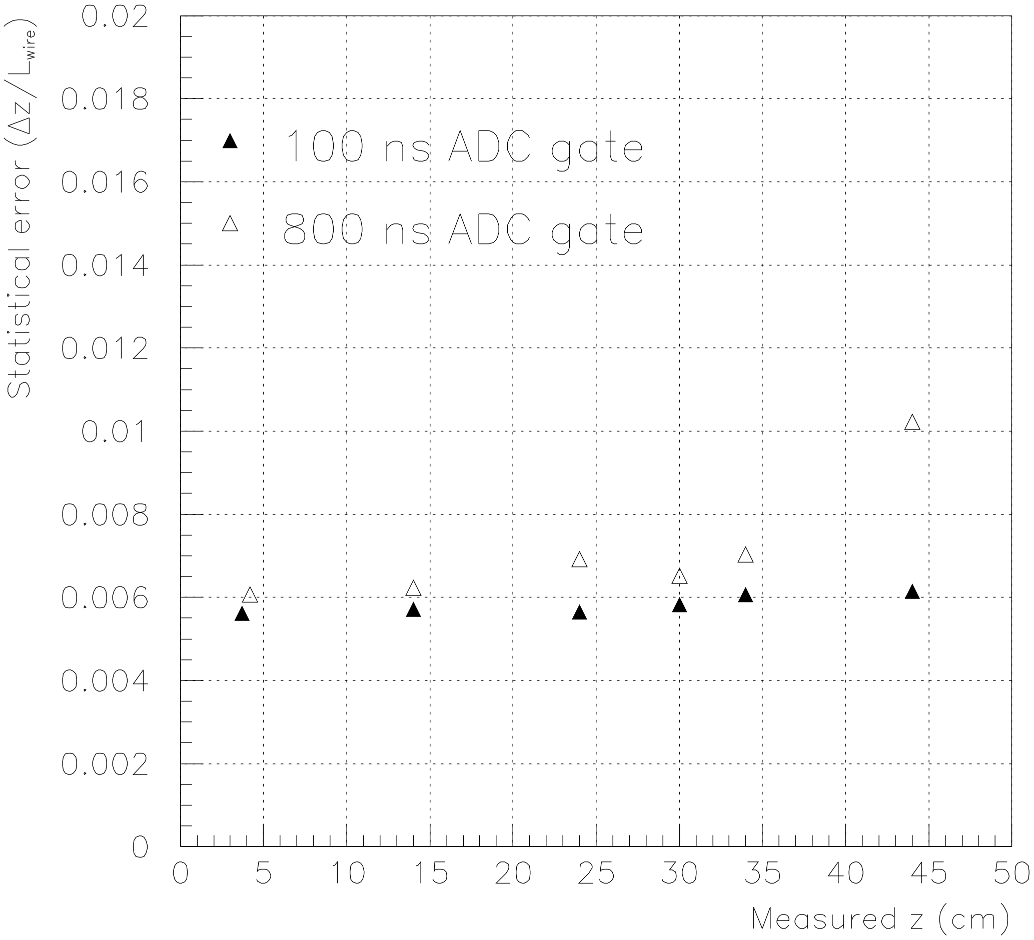

Figure 9: The relative statistical error on the coordinate measurement, due to electronic noise fluctuations, as a function of z at 100 ns and 800 ns ADC gate time (black and white triangles).